Tailored Coumarin Dyes for Photoredox Catalysis: Calculation, Synthesis, and Electronic Properties

Tailored Coumarin Dyes for Photoredox Catalysis: Calculation, Synthesis, and Electronic Properties

Andrea Gualandi, Artur Nenov, Marianna Marchini, Giacomo Rodeghiero, Irene Conti, Ettore Paltanin, Matteo Balletti, Paola Ceroni, Marco Garavelli, and Pier Giorgio Cozzi

ChemCatChem **2021**, *13*, 981 – 989

DOI: 10.1002/cctc.202001690

Tailored Coumarin Dyes for Photoredox Catalysis: Calculation, Synthesis, and Electronic Properties

Andrea Gualandi,*†[a] Artur Nenov,*†[b] Marianna Marchini,[a] Giacomo Rodeghiero,[a],[c] Irene Conti,[a] Ettore Paltanin,[a] Matteo Balletti,[a] Paola Ceroni,*[a] Marco Garavelli,*[b] and Pier Giorgio Cozzi*[a]

[a] Dr. A. Gualandi, Dr. M. Marchini, Dr. G. Rodeghiero, Mr. M. Balletti, Prof. P. Ceroni, Prof. P. G. Cozzi
Dipartimento di Chimica "G. Ciamician",
Alma Mater Studiorum – Università di Bologna
Via Selmi 2, 40126, Bologna, Italy
andrea.gualandi10@unibo.it; piergiorgio.cozzi@unibo.it; paola.ceroni@unibo.it

[b] Dr. A. Nenov, Dr. I. Conti, Mr. E. Paltanin, Prof. M. Garavelli
Dipartimento di Chimica Industriale "T. Montanari",
Alma Mater Studiorum – Università di Bologna
Viale Risorgimento 4, 40136, Bologna, Italy
E-mail: marco.garavelli@unibo.it

[b] Dr. G. Rodeghiero
Cyanagen Srl,
Via Stradelli Guelfi 40/C, 40138, Bologna, Italy

† These authors contributed equally to this work

Abstract: High level time-dependent density functional theory (TD-DFT) computational modeling of coumarin dyes has been exploited for guiding the design of effective photocatalysts (PCs). A library of coumarins were investigated from the theoretical point of view and photophysical/electrochemical properties (absorption and emission spectra, E_{00}, oxidation and reduction potentials) were evaluated. Comparison with literature values reported for a few candidates has been used for assessing the level of theory. On the basis of the results obtained, new strongly reducing PCs [$E_{ox}(PC^{\bullet+}/PC^*)$ = - 2.2 — - 2.0 V vs SCE] were discovered. Through the computational study of structure–properties relationships, a number of coumarins derivatives have been synthesized and evaluated in the pinacol coupling of aldehydes as the model reaction. The new organic photoredox catalysts show experimental photophysical and electrochemical data in accordance with the ones predicted by calculation, with excited state reduction potentials surpassing those of highly reducing transition metal-based PCs. A careful investigation of their behavior as PC has revealed crucial issues that need to be taken into consideration in the general photoredox catalysis, shedding light on the use of these PC in the pinacol, as well as, in other photoredox reactions.

Introduction

In recent years photoredox catalysis has led to the development of interesting new catalytic transformations due to the mild conditions in which operates.[1] Photoredox catalysis has been applied to the synthesis of small molecules,[2] as well as to the preparation of polymers,[3] both in academic and industrial fields.[4] The Renaissance of photoredox catalysis and its rapid advancements were related principally to the use of transition metals complexes as photocatalyst (PC), such as ruthenium[5] or iridium complexes,[6] both capable of absorbing visible light and to initiate electron or energy transfer reactions from their reactive photoexcited states.[7] These photoredox

catalysts were found quite effective due to their photophysical properties such as redox stability, reversible oxidation and reduction processes, and ability to adsorb visible light.[8] Furthermore, their excited states are long lived and they can be engaged in both reductive and oxidative electron transfers. By synthesis it was possible to vary the photophysical properties of ruthenium and iridium complexes,[9] covering a large spectrum of photophysical properties and amplifying their use, particularly when strong reductants or strong oxidants are needed. However, despite their successful use in many reactions, these complexes are expensive and not all are commercially available. In addition, the use of Ru and Ir based photocatalysts presents a concern with regard to their availability and sustainability,[10] as they are among the rarest metals on earth. Furthermore, residual metal traces in the final product can limit their employments, for example for bio-medical applications. To overcome these drawbacks, several alternative PCs were explored in recent years. Organic PC (OPC) families represent a valuable alternative. Several families of organic molecules were studied—including anthracenes,[11] benzophenones,[12] acridiniums,[13] xanthene based dyes,[14] perylene diimides,[15] and many others.[16] Most of the mentioned organic dyes are operating through a reductive quenching pathway generating a strong organic reductant. Making an organic molecule a strong reductant is a difficult task. Murphy described powerful organic reductants able to promote radical coupling and other reactions of substrates with reduction potentials < -1.8 V (vs a saturated calomel electrode, SCE).[17] Unfortunately, these organic reductants are rather unstable and difficult to generate, although an interesting catalytic variant was recently reported.[18] Miyake has developed and studied UV light-absorbing *N*-aryl phenoxazines as strongly reducing metal-free photoredox catalyst for Atom Transfer Radical Polymerization (ATRP),[19] that can access a highly reducing excited state and operate via an oxidative quenching pathway, analogous to the one previously reported for iridium-catalyzed reactions in ATRA reactions.[20] By the guidance of computational methodologies Miyake designed new dyes with interesting properties:[21] (i) strong visible-light absorption (high molar absorptivity); (ii) long-lived excited state; (iii) sufficiently negative excited state reduction potential for the reduction of alkyl bromide,[22] employed as initiators in polymerization reactions; (iv) sufficiently oxidizing, in their oxidized species, for oxidation of the propagating radical; (v) redox reversibility, i.e., stable radical cations or radical anions; (vi) low reorganization energy for the transition from PC* to $PC^{\bullet+}$ and back to ground state PC; and (vii) photoinduced charge-transfer excited states resulting from spatially separated singly occupied molecular orbitals (SOMOs). From this theoretical and experimental work, new organic dyes, *N,N*-diaryldihydrophenazines (PhenN's) and *N*-arylphenoxazines (PhenO's)[23] were reported to have a computationally predicted highly reducing triplet excited states of [$E_{ox}(^2PC^{\bullet+}/^3PC^*) < -2.0$ V vs SCE], together with the capability to adsorb visible light. Beside these dyes, *N*-arylphenothiazine (PTH) derivatives are also interesting and active photoreductants, with have reduction potential in the order of $E_{ox}(PC^{\bullet+}/PC^*)$ = -2.0 — -2.1 V vs. SCE.[24]

We have recently introduced in the field of photoredox catalysis coumarins as new effective photocatalysts.[25] Remarkably, although coumarins have been largely used in many applications,[26] their systematic employment in photoredox reactions has not been explored yet. Coumarins can be accessed by straightforward synthesis[27] that gives the possibility to vary their photophysical and redox properties,[28] allowing to cover a wide range of redox potentials in their ground and excited state. With all these potentialities, we have applied coumarin dyes as powerful photoreductant in pinacol coupling,[25,29,30] replacing the use of iridium complexes for this transformation.[31] In addition, we have shown that a completely different mechanistic picture is operating[25] and that the coumarin dyes, in their excited state, are able to directly reduce carbonyls to the corresponding ketyl radicals. We were interested in tailoring redox and photophysical properties of coumarin dyes by introducing appropriate substituents, for exploring all the possibilities offered by these scaffolds. For this reason, as was recently explored by different authors,[32] we decided to study the photophysical properties of a virtual library of coumarin dyes by the state of the art theoretical investigations. By the analysis of the results, a series of coumarins were prepared and tested in pinacol coupling, chosen as the model reaction. We were able to find suitable in silico candidates, that were revealed to be powerful photoreductant. In addition, by careful investigation of redox potential of the dyes conducted by electrochemistry, we were able to shed light on the ability of specific dyes to promote or not the reaction. The theoretical investigation can be used not only to study and predict photochemical properties of new designed dyes, but also to establish the properties necessary for setting a catalytic photoredox cycle. The investigations reported herein is a full account of our studies.

Results and Discussion

In our previous publications we have reported the intriguing photoredox properties of coumarins bearing a thiophen ring.[25] However, many other coumarins that were tested did not exhibit the desired catalytic activity. It was not clear how to design the coumarin scaffold in order to produce an effective photocatalyst, and more importantly, how the subtle modifications of the electronic structure realized through functionalization affected the photophysical properties. To guide the design and reduce the synthetic efforts, we decided to use an *ab-initio* computational strategy to model the photophysical properties of *on silica modified coumarins derivatives* before their synthesis.

In silico design strategy

Efficient reductive OPCs (Organic Photo Catalysts) have to satisfy the following conditions

a) absorption in the visible (> 400 nm) is preferred over ultraviolet (UV) region of electromagnetic spectrum for a selective excitation of the photocatalyst;
b) high molar absorption coefficients (ε) leads to a more efficient absorption of light;
c) lifetimes beyond the nanosecond range enable the bimolecular collision events (at sufficiently high concentration of the substrate) required for effective electron transfer;
d) photoreactive excited state characterized by a strong reductant ability (highly negative value of E_{ox}*) is required to catalyze reactions with organic substrates featuring high reduction potentials;
e) a sufficiently positive potential value E_{ox} is required to regenerate the photocatalyst for the next catalytic cycle.

A bathochromic shift of the absorption spectrum of UV-absorbing compounds (such as most precursors utilized in the development of OPCs) can be realized in a two-fold manner: (i) by introducing on the chromophore electron-donating and/or -withdrawing functional groups; (ii) by extending the conjugation.[20, 21, 32, 33, 34, 35] Regarding coumarin, it has been demonstrated in the past that the introduction of an electron-donating group (EDG) at position 7, in combination with aromatic group at position 3, induces a bathochromic shift and increases the molar absorption coefficient (see **Figure 1,** for the coumarin system and numerations).[36]

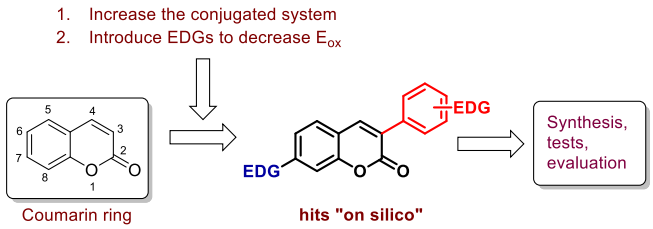

Figure 1. General strategy adopted in the present work.

Blanchard-Desce and co-workers showed that the trend can be amplified by introducing a heterocyclic fused benzenic ring in the position 3.[33] An undesired side effect of the push-pull functionalization, in particular of the use of EWGs, is the increase of the ground state redox potential. To exemplify the dual role of EWGs, we refer to an early work by Bergmark et al. who synthesized a coumarin having CF_3 (an EWG) at position 4 and *N*,*N*-diethylamino (NEt_2, an EDG) in position 7.[37] This push-pull combination is capable of shifting the absorption spectrum to 396 nm, however at the expense of E_{ox} of about 1.2 V (vs SCE), leading to a moderate reported E^*_{ox} = -1.6 V (vs SCE). Therefore, extension of the conjugation should be preferred with respect to push-pull functionalization.

Long-lived (in the μs range) excited states are commonly realized through population of triplet states (^{3}CT) and a general computer-aided-design strategy has been outlined by Kwon.[34] A drawback of this protocol is the loss of reorganization energy associated with

the population of the triplet state from the locally excited (LE) state, which inevitably reduces the reductive power of the catalyst. Recently, Sakata and co-workers reported carbazole based OPCs undergoing photocatalysis directly out of the bright LE state. Their best candidate *N*-ethyl-3,6-bis(dimethylamino)carbazole exhibits an impressive E^*_{ox} = -2.75 V vs. SCE.[35] In our previous study on the photoredox activity of coumarins **1**, **2**, and **5** (**Figure 2**) functionalized with benzene and thiophene rings,[25] we demonstrated that the photoreactive state is the lowest singlet state,[38] as demonstrated by the quenching of the coumarin fluorescence by the organic substrates.

The excited state (S_1) redox potential is related to the ground state (S_0) redox potential through the formula:[16]

$$E^*_{ox} = E_{ox} - E_{00}/nF$$

with *n* is the number of electrons involved in the redox process (here equal to 1) and *F* is the Faraday constant (equal to the unit charge *e* if the employed unit of energy is *eV*). E_{00} is the adiabatic excitation energy given as the difference of the S_0 and S_1 states in their respective minima. The excited state redox potential can be also formulated as the energy inserted in the system upon photoexcitation of the lowest absorption band E_{vert}, diminished by the reorganization energy E_{re} (i.e. $E_{00} = E_{vert} - E_{re}$) and the ground state redox potential E_{ox}.[16]

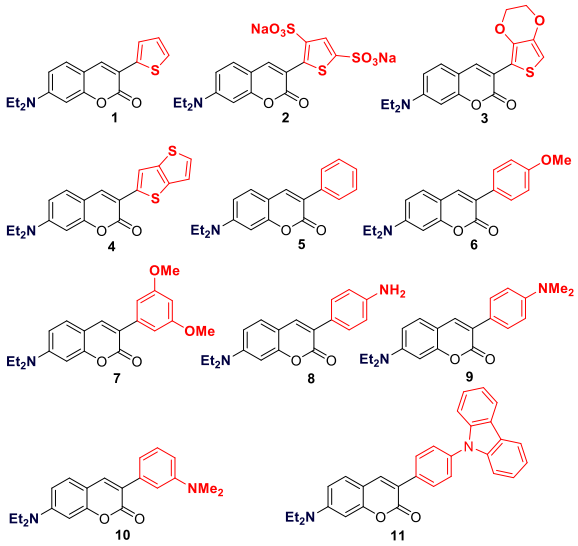

Figure 2. Theoretically investigated coumarin derivatives.

The requirement of absorption in the visible, constrains the adiabatic excitation energy (E_{00}) to values below 3.1 eV.[39] The photoredox potential E_{ox}^* is then tuned by the value of E_{ox},[40] which is associated with the ability of the catalyst to stabilize its radical cation. Thus, for catalysts with similar adiabatic energies E_{00}, those that are easier to oxidize in the ground state will be more strongly reductant in the excited state. Naturally, functionalization with EDGs decreases E_{ox} (**Figure 1**).[32c]

Considering all the above points, we formulate a strategy for in silico design of coumarin derivatives absorbing in the visible and exhibiting high reducing potentials at excited states (**Figure 2**).

Bare coumarin absorbs in the near-UV at 314 nm (maximum of the lowest peak independent of the polarity of the solvent) with a molar absorption coefficient of 0.57 x 10^4 $M^{-1}cm^{-1}$. It exhibits a low fluorescence QY (0.03%) and a few *ps* lifetime in non-polar solvents.[41]

Table 1. Photophysical properties in DMF solution and electrochemical properties ($E_{1/2}$ in V *vs* SCE) in CH_3CN at 298 K of all synthesized coumarins.

	Absorption				Emission			Electrochemistry					
	λ_{abs}		ε x 10^4	f	λ_{em}	Φ_{em}	τ	E_{00}/e		E_{ox} ($PC^{\bullet+}/PC$)		E^*_{ox} ($PC^{\bullet+}/PC^*$)	
Comp.	(nm)		($M^{-1}cm^{-1}$)		(nm)		(ns)	(V)		(V)		(V)	
	exp.	theo.	exp.	theo.	exp.	exp.	exp.	exp.	theo.	exp.	theo.	exp.	theo.
1	427[a]	409	3.30	0.98	497[a]	0.50	3.3[a]	2.66[b]	2.62	+0.79[a]	+0.74	-1.87[c]	-1.88
2	413[a]	398	3.03	1.04	482[a]	0.57	2.9[a]	2.72[b]	2.69	+0.83[a]	+0.75	-1.89[c]	-1.95
3	426	416	2.90	1.01	487	0.65	3.2	2.70	2.61	+0.72[d]	+0.61	-1.98	-1.99
4	442	432	4.25	1.26	515	0.61	3.1	2.59	2.49	+0.81	+0.73	-1.78	-1.76
5	400	377	2.97	0.94	476	0.82	3.0	2.79	2.86	+0.92	+0.88	-1.87	-1.99
6	400	383	2.94	0.96	477	0.60	3.0	2.77	2.78	+0.90	+0.78	-1.87	-2.00
7	402	377	3.35	0.97	475	0.86	2.9	2.78	2.89	+0.93	+0.88	-1.85	-2.00
8	406	394	3.23	0.92	513	0.60	3.5	2.67	2.64	+0.70	+0.60	-1.97	-2.04
9	415	411	2.88	0.90	524	0.52	3.7	2.60	2.56	+0.62	+0.53	-1.98	-2.04
10	398	386	3.07	0.43[e]	480	0.03	2.6	2.78	2.78	+0.71	+0.73	-2.07	-2.05
11	408	389	3.63	1.18	483	0.80	2.5	2.74	2.76	+0.93	+0.87	-1.81	-1.89

[a] Data obtained from ref. [25]; [b] Computed from absorption and emission values as $(\lambda_{max,abs}+\lambda_{max,em})/2$; [c] Computed according to $E^*_{ox} = E_{ox} - E_{00}/e$; [d] Chemically irreversible one-electron transfer process; [e] The low value for the oscillator strength is due to two overlapping absorptions (ΔE = 0.15 eV) with oscillator strengths 0.43 and 0.5 which appear as a single band in the experiment. If both bands are considered the value for f would be in line with the overall trend.

The desired bathochromic shift towards 400 nm is achieved by introducing NEt_2 at position 7, in combination with a (hetero)aromatic ring at position 3 such as phenyl (**5**) and thiophene (**1**, **2**),[42] i.e. effectively extending the conjugated system (**Figure 2**). Phenyl and thiophene achieve the desired red-shift keeping E_{ox} low with values of 0.92 V and 0.79 V vs SCE, respectively.[25] This results in a significant increase in the photoredox potential with reported values of -1.87 V vs SCE for both **1** and **5** (**Table 1**).[25] The aromatic rings offer various possibilities for further functionalization. In particular, we studied the effect of EDGs such as negatively charged groups (SO_3^-, **2**), groups with strong +M effect (OR: **3**, **6**, **7**, NH_2: **8** or NMe_2, **9**, **10**) and fused heteroaromatic rings (thienothiophene, **4**, carbazole, **11**) regarding the fine-tuning of the spectroscopic properties. Our fully *ab initio* calculations (for details regarding the computational protocol see supporting information) predict photoredox potentials around -1.78 — -2.07 V vs SCE for all compounds (except **4**) which can be traced back mainly to the decrease of E_{ox} to values as low as 0.5 V (Table 1). Notably, in the series MeO → NH_2 → NMe_2, E_{ox} decreases by ~0.3 V, facilitated by the ability of stronger EDGs to stabilize the positive charge more effectively.
Exemplarily, **Figure 3**, top, compares the electrostatic potential (ESP)-mapped electronic density of the radical cation for coumarin functionalized with a phenyl (**5**) and with a 4-dimethylamino phenyl (**9**) ring.[43] As can be seen, the additional EDG leads to a more equilibrated distribution of the charge in the molecule. At the same time, the introduction of an EDG produced a red shift, as a consequence, E_{00} decreases by ~0.2 V (**Table 1**). Specifically, the ESP-mapped electronic densities for the ground and excited state of the neutral forms of **5** and **9** (**Figure 3**, center and bottom) demonstrate that the intramolecular charge transfer is enhanced in the first excited state. Notably, its direction is inverted in **9**. Thus, we note a subtle interplay between E_{ox} and E_{00} which imposes constraints on the values that the excited state redox potential E^*_{ox} can adopt.

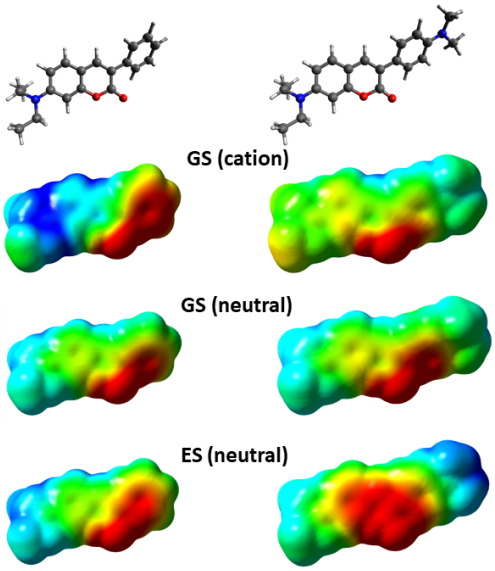

Figure 3. Electrostatic potential (ESP)-mapped electronic density for the radical cation (top) ground state (center) and first excited state (bottom) of compounds **5** (left) and **9** (right). Red and blue color indicate positive and negative values of the ESP, respectively. For the neutral species the ESP maps are plotted with limits [-0.05 : +0.05] a.u., whereas for the cations the ESP maps are plotted with limits [+0.05 : +0.15] a.u.

Design synthetic strategy for DFT calculated coumarins

Based on the results obtained by the in-silica screening, new promising compounds were selected, synthesized, and used as photocatalysts in a model reaction in order to test their efficiency, and the affordability of the calculations. However, as stressed it is possible to verify the comparison between the theoretical and experimental data of coumarins, as in the case of **1**, **2** and **5,** coumarins, that were already found as good catalysts for pinacol coupling reaction,[25] and that exhibit the extreme accuracy of the computational calculations.
The synthesis of the selected candidates was performed through different synthetical approaches.
In the case of coumarin derivatives **6**, **7**, **9**, and **10**, a Suzuki coupling of 3-bromo-coumarin derivative **14** with corresponding boronic acid was required (**Scheme 1**). Compound **14**,[44] was prepared in an excellent yield through a Knoevenagel condensation of 4-(diethylamino)salycilaldehyde (**12**) with diethyl malonate, followed by acid hydrolysis/decarboxylation step to gives **13**, and a

subsequent treatment with Br_2. Boronic acids not commercially available were synthesized in good yields using a classic protocol reported in literature (see SI, for details).

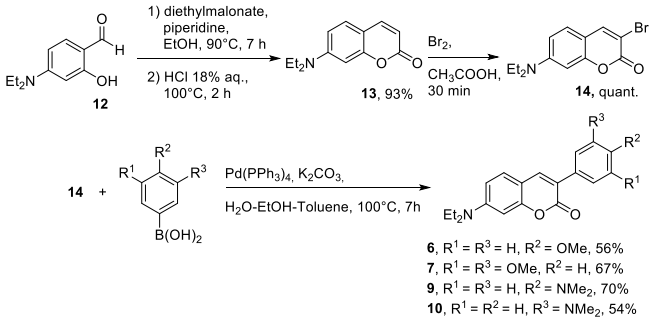

Scheme 1. Synthesis of coumarins **6**, **7**, **9**, **10** by Suzuki Miyura cross coupling reaction.

In the case of compound **8** the synthesis was carried out in three steps including a nitration of benzeneacetonitrile,[45] the Knoevenagel condensation of compound **15** with **12** and a subsequent reduction of the nitro group (**Scheme 2**).[46]

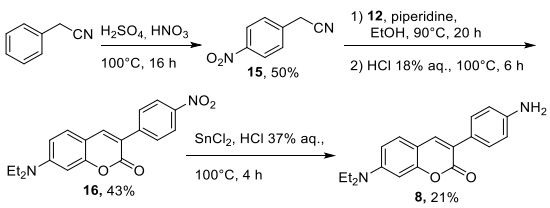

Scheme 2. Synthesis of coumarin **8**.

3, 4 and **11**, were obtained using cross coupling reactions with appropriate conditions and reagents, as depicted in **Scheme 3**. For the compounds **3** and **11**, general conditions of Suzuki coupling were employed starting from commercially available or easily prepared aryl boronic acids (See SI for details). The derivative **4** was obtained by CH activation strategy[47] as reported in literature. In all cases, coumarins were isolated in satisfactory yields.

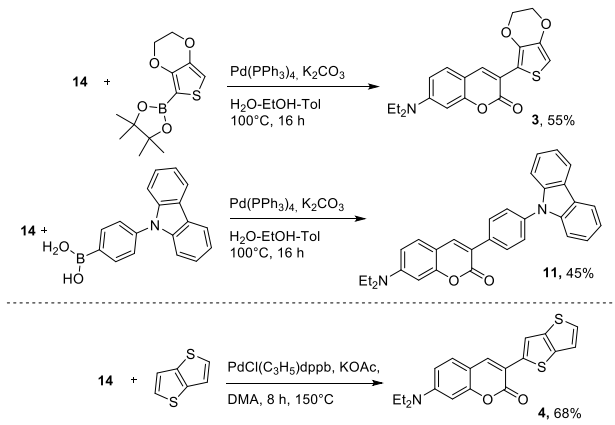

Scheme 3. Synthesis of coumarins **3**,**11,** and **4**.

Use of coumarins synthesized in the pinacol coupling reaction

With all the desired derivatives in our hands, pinacol coupling of 4-chlorobenzaldehyde **17** was selected as model reaction,[25] in order to compare the reduction ability of all the synthesized derivatives.

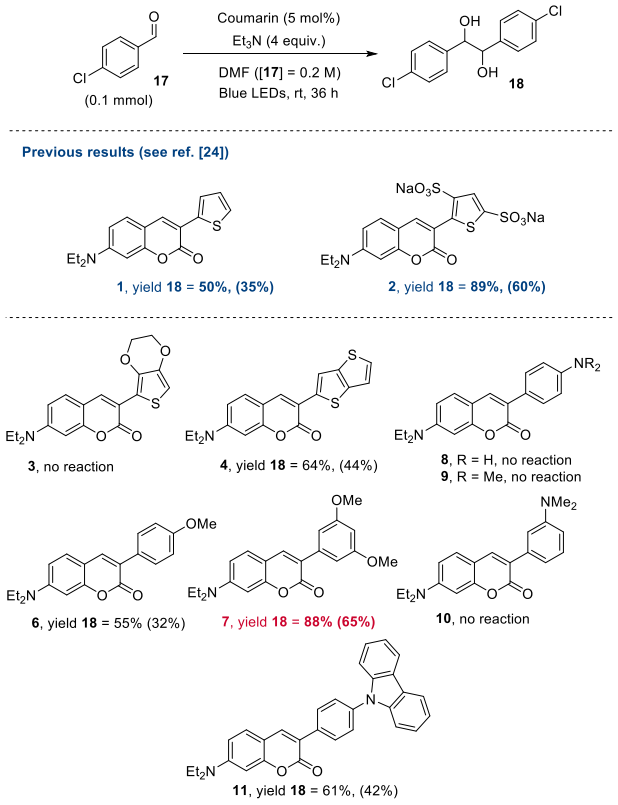

Scheme 4. Comparison between first described coumarin dyes and new synthetized coumarin dyes (yields evaluated by ^{1}H-NMR). Isolated yields after chromatographic purification given in parenthesis.

To our surprise, although the reduction potentials were quite high for almost all derivatives prepared, the results were quite disappointing. Coumarin **7** provided the product **18** in yield of 88%, a value comparable to the best photocatalysts **2**.[25] All the amino derivatives **8**-**10** were inactive, as well the electron rich substrate **3**. Differently, the electron rich compounds **4** and **11** showed a reduced reactivity. Clearly, despite the redox properties, the catalytic cycle of the photoredox catalyst was in same way hampered. A detailed analysis of the catalytic cycle, and of all data were crucial in order to understand the failure, and to the reprojection of experiments. The proposed catalytic cycle, that is following the proposals discussed in publication by Rueping[31] and us[25] is reported in **Figure S8** in SI.

The catalytic cycle of photoredox pinacol coupling occurs by single electron transfer from the photoexcited coumarin PC* to the chlorobenzaldehyde. The related studies and Stern-Volmer analysis were fully described in our previous article.[25] The electron transfer generates the radical cation of the coumarin dye $PC^{\bullet+}$ and the ketyl radical which undergoes dimerization providing the diol **18**. As stressed by Rueping and by us, it is important to highlight the role played by the oxidized form of the sacrificial reductant, in order to favor the endergonic pinacol coupling activation of aldehyde. The sacrificial reductant, triethylamine, is in charge of reducing the coumarin radical cation, and restore the coumarin in its ground state. By our calculations, and by the experimental value of the registered ground state oxidation potential of coumarins (see further discussions), the oxidation potential of the compounds **3**, **8**, **9,** and **10** were found inferior to those of Et_3N (0.91 V vs SCE, see **Figure S5** in SI for more details). Therefore, the inefficient reaction observed with some of the coumarins prepared could be ascribed to their low oxidation potential which results in the inability of Et_3N to close the catalytic cycle. In order to test our hypothesis and found another suitable sacrificial reductant for the reaction, an inspection of table of sacrificial agents used in photoredox catalytic reactions[22,48] was conducted. After having discarded suitable but insoluble sodium ascorbate, and various acid derivatives,[49] our attention was drawn by commercially available 1,3-dimethyl-2-phenyl-2,3-dihydro-1H-benzo[d]imidazole (BIH), a derivative widely used as sacrificial agent in photoredox reduction of α-haloketones,[50] in the ring opening of cyclopropyl ketones,[51] and in the photocatalytic reduction of CO_2.[52] According to the literature, BIH shows an oxidation potential $E(BIH^+/BIH)$ of +0.33V vs SCE in CH_3CN.[53] The oxidation potential is in all cases inferior to the oxidation potential $E(PC^{\bullet+}/PC)$ and

successful reaction with this sacrificial agent was expected. Therefore, the model pinacol coupling was tested in the presence of BIH as reducing agent. Contrary to our expectation, the conversion was absent in all the cases. The addition of oxalic acid, as Brønsted acid, to improve the efficiency of the photoredox coupling reaction, was reported by Rueping et al.[31] The addition of a Brønsted acid was found crucial in order to improve the pinacol coupling of ketones, and oxalic acid, among all the derivatives employed, gave the better conversion. The reaction involved the concerted shift of a single electron and a single proton (proton-coupled electron transfer (PCET) reactions.[54] Different photoredox reactions in which ketyl radical intermediates were formed through Brønsted acids activations were reported.[55] In the reaction performed with BIH, the absence of a Brønsted acid was probably responsible for the observed failures, as the redox potential of chlorobenzaldehyde was too negative for all the coumarins employed. On the other hand, aldehydes are very weakly basic requiring strong acids to generate the corresponding proto-oxocarbenium ions.[56] However, the joint action of Brønsted acids and photo reductants could facilitate efficient ketyl formation through a concerted PCET reaction scheme. On the basis of this hypotheses the addition of oxalic acid in the reaction mixture was evaluated and Scheme **5** reports the collected results.

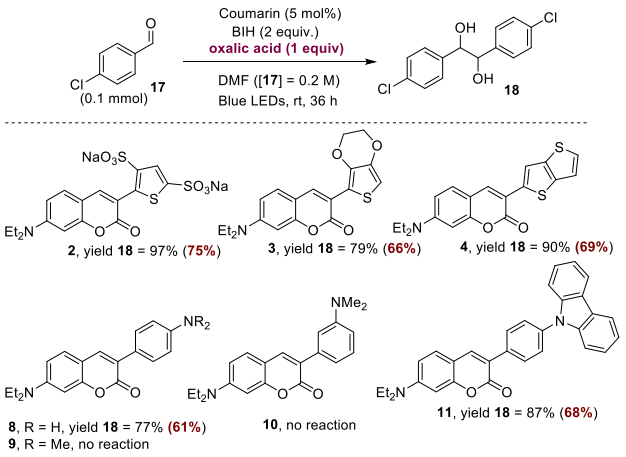

Scheme 5. Pinacol coupling of 4-chlorobenzaldehyde with different coumarins dyes in the presence of BIH as sacrificial reductant. (conversion evaluated by ^{1}H-NMR). Isolated yields given after chromatographic purification given in parenthesis.

Gratifyingly, with most of the new photocatalysts we observed a quite good conversion. The lacking of reactivity observed with the photocatalyst **9** and **10** could be attributed in part to a photo-oxidative degradation, reported for organic photocatalyst under photoredox conditions.[57] Indeed, upon 24 hours of irradiation of the reaction mixture, 60% of the photocatalyst **9** can be recovered but no conversion was detect (**Figure S5**). The new conditions were also tested for the photocatalyst **2** described in our preliminary investigation, and to our delight, the new conditions afforded with the established photoredox catalyst quite high yields. Preliminary investigations with different Brønsted acids shown that phosphoric acids as well as thioureas could be useful molecules in order to promote the pinacol coupling, hoping for a stereoselective variant that will be investigated in near future.

Photophysical and electrochemical properties and comparison with computational results

Among all the synthesized coumarins, four of them were chosen to be representative for the category (see SI for detailed information). Figure **4** reports the absorption and emission spectra of the selected coumarins: the absorption maxima are between 400 and 430 nm and the shape of the band is similar for all the species. The emission maxima are spread over a wider range of wavelengths, between 476 and 524 nm and the emission spectra do not present any vibronic feature.

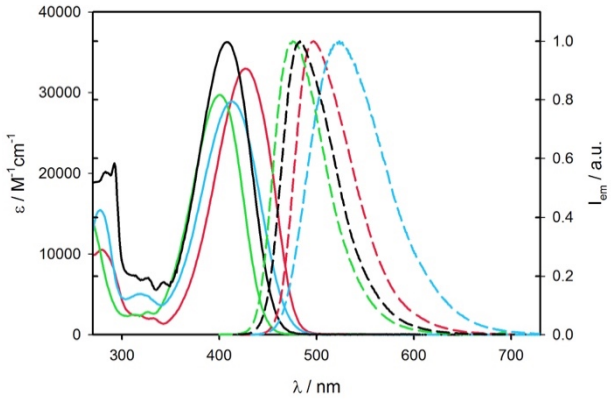

Figure 4. Absorption (left, solid lines) and emission spectra (right, dashed lines) of **1** (red line), **5** (green line), **9** (light-blue line) and **11** (black line) in DMF solution at 298 K. λ_{ex} = 400 nm.

The cyclic voltammetry of the synthesized coumarins (a selection is reported in **Figure 5**) shows chemically reversible one-electron transfer process with E_{ox} value from +0.62 V (vs SCE) to +0.93 V (vs SCE). In the case of coumarins **8**, **9** and **10** two reversible oxidation processes are observed, and this can be attributed to the presence of two amine functions in the coumarin skeleton. The only exception is coumarin **3**, which shows a chemically irreversible oxidation process (see **Figure S2**), likely due to the dioxythiophene substituent that can easily undergo electro-oxidative polymerization.[58]

through **11**. We note the excellent agreement with respect to the adiabatic energies E_{00} (black lines in **Figure 6**) which reinforces

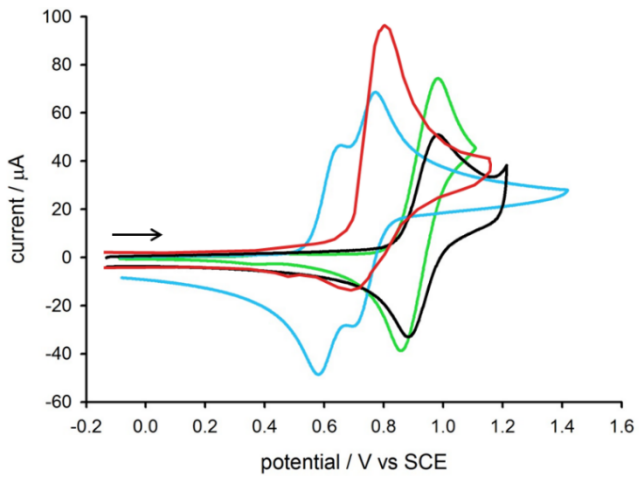

Figure 5. Cyclic Voltammetry of an argon-purged solution of **1** (1.4 mM, red line), **5** (1 mM, green line), **9** (1 mM, light-blue line) and **11** (1 mM, black line) in CH_3CN in the presence of 0.1 M tetraethylammonium hexafluorophosphate ($TEAPF_6$). Scan rate=0.2 Vs^{-1}; working electrode: glassy carbon. The arrow shows the scanning direction of the cyclic voltammetry diagrams.

Figure 6 compares the theoretical and experimental values for the photophysical and electrochemical properties of coumarins **1** the versatility of the selected DFT functional M06[59] and, in particular, the suitability of the Minnesota functional to describe excited states where long-range correlation effects are of crucial importance. The ground state redox potentials E_{ox} (red lines in **Figure 6**) are systematically underestimated by ca. 0.05 V (except **10**) which rationalizes the slightly overestimated values for the photoredox potential E^*_{ox} (blue lines in **Figure 6**). Overall, the similar trend exhibited by the computed and measured data sets is an attestation for the utilized fully *ab-initio* protocol (for details see SI).

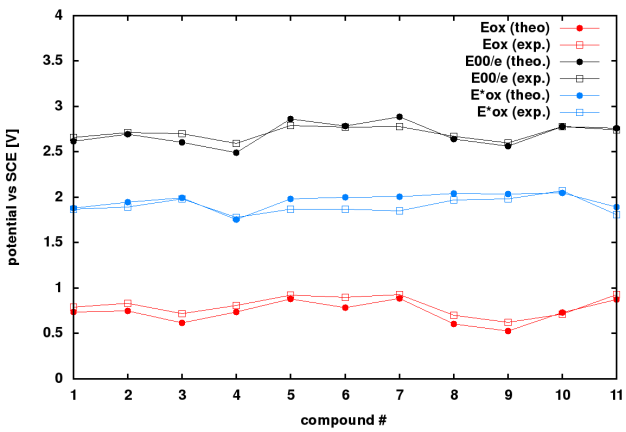

Figure 6. Measured (squares) and calculated (dots) E_{00}, E_{ox} and E^{*}_{ox} for all synthesized coumarins in DMF solution at 298 K.

Moreover, some points related to the photophysical properties can be added. The formation of twisted intramolecular charge transfer (TICT) in the excited state could be the reason for the non-unity yield of the emission (Φ_{em} in Table 1, in particular for **9** Φ_{em} = 3%) as well as for the lack of catalytic activity in some coumarins.

Liu and co-workers showed that coumarins functionalized with NR_2 (R = H, Me, Et) exhibit a TICT (thermodynamically stable in polar solvents) that can be reached over a barrier which decreases with the increasing polarity of the solvent.[60] Based on extensive computational and experimental analysis the authors suggested to replace NR_2 with the four-membered *N*-containing ring azetidine to enhance the brightness. Xu and co-workers demonstrated that the tri-membered aziridine outperforms azetidines.[61] Finally, we note that enclosing the *N*-atom in a fused ring formation would naturally inhibit the formation of TICT. It has been demonstrated experimentally that this type of functionalization decreases E_{ox} by 0.2 V,[37] thus potentially increasing the value of E_{ox}* to -2.3 V vs SCE.

Conclusion

In conclusion, new photoredox coumarins catalysts were accessed through catalyst design and investigations carried out with combined experimental studies and density functional theory (DFT) calculations. The redox and photophysical properties of the newly designed catalysts were completely investigated. The theoretical predictions and experimental results are in quite good agreement, highlighting the good selection of level of theory and functional used for this investigation. The newly designed catalysts were tested in pinacol coupling reaction of aldehydes, as representative photoredox reaction for evaluated the performance of the catalyst. By careful analysis of the reaction outcome, redox potentials, and electrochemistry of the obtained coumarins, we have fully defined the criteria for the reaction and shed light on the catalytic cycle. In addition, we have employed for the reaction other sacrificial agents, such as BIH, showing the limitation of the process. All insights gained in the analysis of experimental data can clarify the role of oxidation and reduction potentials of the photocatalyst, both in ground and in excited state, helping to interpret and guide the development of similar photoredox catalytic investigations.

Acknowledgements

Prof G. Bergamini is acknowledged for discussions. Cyanagen srl is acknowledged for financial support for this research (PhD fellowship to G. R) and for the generous supplying of coumarins dyes. National PRIN 2017 projects (ID: 20174SYJAF, SURSUMCAT and ID: 20172M3K5N, CHIRALAB) are acknowledged for financial support of this research. Partial financial support from Bologna University is acknowledged. We thank Mr. Francesco Calogero for perform some catalytic tests.

Keywords: Photoredox • DFT Calculation • Organic Dyes • Coumarins • Pinacol coupling

[1] a) J. M. R. Narayanam, C. R. J. Stephenson, *Chem. Soc. Rev.* **2011**, 40, 102 – 113; b) C. K. Prier, D. A. Rankic, D. W. C. MacMillan, *Chem. Rev.* **2013**, *113*, 5322-5363; c) M. H. Shaw, J . Twilton, D. W. C. MacMillan *J. Org. Chem.* **2016**, *81*, 6898 – 6926; d) T. R. Blum, Z. D. Miller, D. M. Bates, I. A. Guzei, T. P. Yoon, *Science* **2016**, *354*, 1391 – 1395.

[2] R. C. McAtee, E. J. McClein, C. R. J. Stephenson, *Trends Chem.* **2019**, *1*, 111-125.

[3] B. P. Fors, C. J. Hawker, *Angew. Chem.* **2012**, *124*, 8980 – 8983; *Angew. Chem. Int. Ed.* **2012**, *51*, 8850 – 8853.

[4] M. K. Bodos, E. Pinnard, J. A. Murphy, *Beilstein J. Org. Chem.* **2018**,*14*, 2035 – 2064.

[5] S. Angerani, N. Winssinger, *Chem. Eur. J.* **2019**, *25*, 6661 – 6672, and ref. cited therein.

[6] M.-A. Tehfe M. Lepeltier, F. Dumur, D. Gigmes, J.-P. Fouassier, J. Lalevée, *Macromol. Chem. Phys.* **2017**, *218*, 1700192, and ref. therein.

[7] a) V. Balzani, G. Bergamini, P. Ceroni, *Angew. Chem.* **2015**, *127*, 11474 – 11492; *Angew. Chem. Int. Ed.* **2015**, *54*, 11320-11337; b) V. Balzani, G. Bergamini, P. Ceroni, *Rend. Fis. Acc. Lincei* **2017**, *28*, 125 – 142.

[8] a) D. M. Arias-Rotondo, J. K. McCusker, *Chem. Soc. Rev.*, **2016**, *45*, 5803 – 5820; b) L. Buzzetti, G. E. M. Crisenza, P- Melchiorre, *Angew. Chem.* **2019**, 131, 3768-3786; *Angew. Chem. Int. Ed.* **2019**, *58*, 3730 – 3747.

[9] Photochemistry and photophysics of coordination compounds I (Eds.: V. Balzani, S. Campagna), Springer, **2007.**

[10] J. R. Ludwig, C. S. Schindler, *Chem* **2017**, *2*, 313 – 316.

[11] a) M. Nakamura, R. Dohno, T. Majima, *J. Org. Chem.* **1998**, *63*, 6258 – 6265; b) S. Hintz, J. Mattay, R. van Eldik, W.-F. Fu, *Eur. J. Org. Chem.* **1998**, 1583 – 1596; c) G. Pandey, R. Laha, *Angew. Chem.* **2015**, *127*, 15088-15092; *Angew. Chem. Int. Ed.* **2015**, *54*, 14875-14879.

[12] a) C. Manfrotto, M. Mella, M. Freccero, M. Fagnoni, A. Albini, *J. Org. Chem.* **1999**, *64*, 5024 – 5028; b) D. Dondi, S. Protti, A.; Albini, S. M. Carpio, M. Fagnoni, *Green Chem.* **2009**, *11*, 1653 – 1659; c) J .-B. Xia, C. Zhu, C. Chen, *J. Am. Chem. Soc.* **2013**, *135*, 17494-17500.

[13] a) H. Kotani, K. Ohkubo, S. Fukuzumi, *J. Am. Chem. Soc.* **2004**, *126*, 15999 – 16006; b) K. Ohkubo, K. Mizushima, R. Iwata, K. Souma, N. Suzuki, S. Fukuzumi, *Chem. Commun.* **2010**, *46*, 601 – 603. c) M. Xiang, Q .-Y. Meng, J .-X. Li, Y.-W. Zheng, C. Ye, Z.- J. Li, B. Chen, C.-H. Tung, L.-Z. Wu, *Chem.—Eur. J.* **2015**, *21*, 18080 – 18084.

[14] T. Keshari, V. K. Yadav, V. P. Srivastava, L. D. S. Yadav, *Green Chem.* **2014**, *16,* 3986 – 3992; b) Yang, W.; Yang, S.; Li, P.; Wang, L. *Chem. Commun.* **2015**, *51*, 7520-7523; c) A. U. Meyer, S. Jäger, D. P. Hari, B. König, *Adv. Synth. Catal.* **2015**, *357*, 2050 – 2054.

[15] a) M. Marchini, A. Gualandi, L. Mengozzi, P. Franchi, M. Lucarini, P. G. Cozzi, *Phys. Chem. Chem. Phys.* **2018**, *20*, 8071 – 8076; b) C. Rosso, G. Filippini, P. G. Cozzi, A. Gualandi, M. Prato, *ChemPhotoChem* **2019**, *3*, 193 – 197; and ref. therein.

[16] N. A. Romero, D. A. Nicewicz, *Chem. Rev.* **2016**, *116*, 10075 – 10166.

[17] J. A. Murphy, *J. Org. Chem.* **2014**, *79*, 3731 – 3746.

[18] S. Rohrbach, R. S. Shah, T. Tuttle, J. A. Murphy, *Angew. Chem.* **2019**, *131*, 11576 – 11580; *Angew. Chem. Int. Ed.*, **2019**, *58*, 11454 – 11458.

[19] R. M. Pearson, C. H. Lim, B. G. McCarthy, C. B. Musgrave, G. M. Miyake, *J. Am. Chem. Soc.* **2016**, *138*, 11399 – 11407.

[20] C.-J. Wallentin, J. D. Nguyen, P. Finkbeiner, C. R. J. Stephenson, *J. Am. Chem. Soc.* **2012**, *134*, 21, 8875 – 8884.

[21] For a recent work, see: S. M. Sartor, C. H. Chrisman, R. M. Pearson, G. M. Miyake, *J. Phys. Chem. A*, **2020**, *124*, 5, 817 – 82; b) B. L. Buss, C.-H. Lim, G. M. Miyake, *Angew. Chem.* **2020**, 132, 3235 – 3243; *Angew. Chem. Int. Ed.* **2020**, *59*, 3209 – 3217.

[22] H. G. Roth, N. A. Romero, D. A. Nicewicz, *Synlett* **2016**, *27*, 714-723.

[23] For an account, see: D. A. Corbin, C. H. Lim, G. M. Miyake, *Aldrichimica Acta* **2019**, *52*, 9 – 23; and ref. therein.

[24] a) H. Gong, Y. Zhao, X. Shen, J. Lin, M. Chen, *Angew. Chem.* **2018**, *130*, 339 – 343; *Angew. Chem. Int. Ed.* **2018**, *57*, 333 – 337; b) N. J. Treat, H. Sprafke, J. W. Kramer, P. G. Clark, B. E. Barton, J. R. de Alaniz, B. P. Fors, C. J. Hawker, *J. Am. Chem. Soc.* **2014**, *136*, 16096 – 16101; c) K. Jiang, S. Han, M. Ma, L. Zhang, Y. Zhao, M. Chen, *J. Am. Chem. Soc.* **2020**, *142*, 7108 – 7115.

[25] A. Gualandi, G. Rodeghiero, E. Della Rocca, F. Bertoni, M. Marchini, R. Perciaccante, T. P. Jansen, P. Ceroni, P. G. Cozzi, *Chem. Commun.* **2018**, *54*, 10044-10047.

[26] a) H. Li, L. Cai, J Li, Y. Hu, P. Zhou, J. Zhang, Dyes Pigm **2011**, *91*, 309 – 316; b) B. B. Raju, T. S. Varadarajan; *Laser Chem.* ***1995***, *16*, 109 – 120; c) M. Fujiwara, N. Ishida, M. Satsuki, S. Suga, *J. Photopolym. Sci. Technol.* **2002**, *15*, 237 – 238; d) K. Hara, Z.-S. Wang, T. Sato, A. Furube, R. Katoh, H. Sugihara, Y. Dan-oh, C. Kasada, A. Shinpo, S. Suga, *J. Phys. Chem. B* **2005**, *109*, 15476 – 15482.

[27] S.-M. Yang, C.-Y. Wang, C.-K. Lin, P. Karanam, G. M. Reddy, Y.-L. Tsai, W. Lin, *Angew. Chem.* **2018**, *130*, 1684 – 1688; *Angew. Chem. Int. Ed.* **2018**, *57*, 1668 – 1672, and ref. cited therein

[28] a) A. K. Sanap, K. K. Sanap, G. S. Shankarling, *Dyes Pigm.* **2015**, *120*, 190-199; b) M. Ozkütük, E. Ipek, B. Aydıner, S. Mamas, Z. Seferoglu, *J. Mol. Struct.* **2016**, *1108*, 521 – 532.

[29] For a pioneering work on light-mediated pinacol coupling, see: G. Ciamician, P. Silber, *Ber. dtsch. Chem. Ges.* **1900**, *33*, 2911 – 2913; For a direct intermolecular ketyl radical coupling in the field of photoredox chemistry, see: E. Fava, A. Millet, M. Nakajima, S. Loescher, M. Rueping, *Angew. Chem.* **2016**, *128*, 6888 – 6891; *Angew. Chem. Int. Ed.* **2016**, *55*, 6776 – 6779. For an enantioselective protonation of activated ketoimines and ketone, through formation of ketyl radical, see: L. Lin, X. Bai, X. Ye, X. Zhao, C.-H. Tan, Z. Jiang, *Angew. Chem.* **2017**, *129*, 14030 – 14034; *Angew. Chem. Int. Ed.* **2017**, *56*, 13842 – 13846. For other photocatalytic pinacol coupling: a) C.-Ming Wang, P.-J. Xia, J.-A. Xiao, J. Li, H.-Y. Xiang, X.-Q. Chen, *J. Org. Chem.* **2017**, *82*, 3895 – 3900; b) L. J. Rono, H. G. Yayla, Y. Wang, M. F. Armstrong, R. R. Knowles, *J. Am. Chem. Soc.* **2013**, *135*, 17735 – 17738; c) M. Zhang, W. D. Rouch, R. D. McCulla, *Eur. J. Org. Chem.* **2012**, 6187 – 6196. For an organocatalytic reductive coupling of aldehydes with 1,1-diarylethylenes using an in situ generated pyridine-boryl radical, see: J. Cao, G. Wang, L. Gao, X. Cheng, S. Li, *Chem. Sci.* **2018**, 9, 3664 – 3671.

[30] For a reductive coupling of carbonyl and imine bonds driven by visible light by the use of perylene as a simple photoredox catalyst, see: S. Okamoto, K. Kojiyama, H. Tsujioka, A. Sudo, *Chem. Comm.* **2016**, *52*, 11339 – 11342. For the use of polymeric organic material as a photoredox catalyst to promote pinacol coupling of aryl-aldehydes with visible light, see: a) W. D. Rouch, M. Zhang, R. D. McCulla, *Tetrahedron Lett.* **2012**, *53*, 4942 – 4945; b) T. Shibata, A. Kabumoto, T. Shiragami, O. Ishitani, C. Pac, S. Yanagida *J. Phys. Chem.*, **1990**, *94*, 2068 – 2076. It is worthy to mention that in this case and also with

perylene the reaction is occurring by a reductive photocatalytic cycle, in which the $PC^{\bullet-}$ is the reductant, and the photo redox mechanism is different from the coumarin dyes (PC = photocatalyst).

[31] M. Nakajima, E. Fava, S. Loescher, Z. Jiang, M. Rueping, *Angew. Chem.* **2015**, *127*, 8952 – 8954; *Angew. Chem. Int. Ed.* **2015**, *54*, 8828 – 8832.

[32] a) S. M. Sartor, Y. M. Lattke, B. G. McCarthy, G. M. Miyake, N. H. Damrauer, *J. Phys. Chem. A* **2019**, *123*, 4727-4736; b) S. M. Sartor, B. G. McCarthy, R. M. Pearson, G. M. Miyake, N. H. Damrauer, *J. Am. Chem. Soc.* **2018**, *140*, 4778-4781; c) B. G. McCarthy, R. M. Pearson, C. H. Lim, S. M. Sartor, N. H. Damrauer, G. M. Miyake, *J. Am. Chem. Soc.* **2018**, *140*, 5088-5101; d) E. Speckmeier, T. G. Fischer, K. Zeitler, *J. Am. Chem. Soc.* **2018**, *140*, 15353-15365; e) B. L. Buss, C.-H. Lim, G. M. Miyake, *Angew. Chem.* **2020**, *132*, 3235-3243; *Angew. Chem. Int. Ed.* **2020**, *59*, 3209-3217; f) D. Liu, M.-J. Jiao, Z.-T. Feng, X.-Z. Wang, G.-Q. Xu, P.-F. Xu, *Org. Lett.* **2018**, 20, 5700-5704.

[33] M. Klausen, V. Dubois, G. Clermont, C. Tonnelé, F. Castet, M. Blanchard-Desce, *Chem. Sci.* **2019**, *10*, 4209-4219.

[34] V. K. Singh, C. Yu, S. Badgujar, Y. Kim, Y. Kwon, D. Kim, J. Lee, T. Akhter, G. Thangavel, L. S. Park, J. Lee, P. C. Nandajan, R. Wannemacher, B. Milián-Medina, L. Lüer, K. S. Kim, J. Gierschner, M. S. Kwon. *Nat. Cat.* **2018**, *1*, 794-804.

[35] R. Matsubara, T. Yabuta, U. Md Idros, M. Hayashi, F. Ema, Y. Kobori, K. Sakata, *J. Org. Chem.* **2018**, 83, 16, 9381-9390.

[36] a) J. P. Olson, H.-B. Kwon, K. T. Takasaki, C. Q. Chiu, M. J. Higley, B. L. Sabatini, G. C. R. Ellis-Davies, *J. Am. Chem. Soc.* **2013**,*135*, 5954-5957. b) L. Fournier, I. Aujard, T. Le Saux, S. Maurin, S. Beaupierre, J.-B. Baudin, L. Jullien, *Chem.–Eur. J.*, **2013**, *19*, 17494-17507. c) Y. Chitose, M. Abe, K. Furukawa, C. Katan, *Chem. Lett.*, **2016**, *45*, 1186-1188.

[37] G. Jones, II, S. F. Griffin, C. Choi, W. R. Bergmark, *J. Org. Chem.* **1984**, *49*, 2705-2708.

[38] Frontier orbitals HOMO and LUMO of the lowest excited state (S1) of all compounds are shown in the SI (Fig. S5)

[39] We note that it is sufficient that the absorption cross section of the catalyst exhibits a tail in the Visible, whereas absorption maximum λ_{max} could fall within the near-UV.

[40] Photoredox catalysis mechanisms involving triplet states entail an additional reduction of E^{*}_{ox} due to the reorganization energy associated with the dark state; see references [20], [22], [32] and [34].

[41] C. M. Krauter, J. Möhring, T. Buckup, M. Pernpointner, M. Motzkus, *Phys. Chem. Chem. Phys.* **2013**, *15*, 17846.

[42] P. Kotchapadist, N. Prachumrak, T. Sunonnam, S. Namuangruk, T. Sudyoadsuk, T. Keawin, S. Jungsuttiwong, V. Promarak, *Eur. J. Org. Chem.* **2015**, 496-505.

[43] ESP-mapped electronic densities for the remaining compounds are shown in the SI (Fig. S6).

[44] H. Sun, H. Guo, W. Wu, X. Liu, J. Zhao, *Dalton Transactions* **2011**, *40*, 7834-7841.

[45] G. R. Robertson, *Org. Synth.* **1922**, *2*, 57.

[46] B. Zhang, C. Ge, J. Yao, Y. Liu, H. Xie, J. Fang, *J. Am. Chem. Soc.* **2015**, *137*, 757-769.

[47] T. M. Ha Vuong, D. Villemin, H.-H., Nguyen, T. T. Le, T. T. Dang, H. Nguyen, *Chem. Asian J.* **2017**, *12*, 2819-2826.

[48] O. R. Luca, J. L. Gustafson, S. M. Maddox, A. Q. Fenwick, D. C. Smith, *Org. Chem. Front.* **2015**, *2*, 823-848.

[49] G. Magagnano, A. Gualandi, L. Mengozzi, M. Marchini, P. Ceroni, P. G. Cozzi, *Chem. Commun.* **2017**, *53*, 1591-1594.

[50] D. D. Tanner, J. J. Chen, *J. Org. Chem.* **1989**, *54*, 3842–3846.

[51] D. D. Tanner, J. J. Chen, C. Luelo, P. M. Peters; *J. Am. Chem. Soc.*, **1992**, *114*, 713-717.

[52] a) Y. Tamaki, K. Koike, T. Morimoto, O. Ishitani; *J. Cat.*, **2013**, *304*, 22–28; b) D. Hong, Y. Tsukakoshi, H. Kotani, T. Ishizuka, T. Kojima, *J. Am. Chem. Soc.* **2017**, *139*, 6538–6541.

[53] Y. Yamazaki, H. Takeda, O. Ishitani, *J. Photochem. Photobiol. C*, **2015**, *25*, 106 – 137.

[54] a) T. J. Meyer, M. H. V. Huynh, H. H. Thorp, *Angew. Chem.* **2007**, *119*, 5378 – 5399; *Angew. Chem. Int. Ed.* **2007**, *46*, 5284 – 5304; b) J. Stubbe, D. G. Nocera, C. S. Yee, M. C. Y. Chang, *Chem. Rev.* **2003**, *103*, 2167 – 2202; c) V. R. I. Kaila, M. I. Verkhovsky, M. Wikstrçm, *Chem. Rev.* **2010**, *110*, 7062 – 7081; d) E. C. Gentry, R. R. Knowles, *Acc. Chem. Res.* **2016**, *49*, 1546 – 1556; e) H. G. Yayla, R. R. Knowles, *Synlett* **2014**, *25*, 2819 – 2826.

[55] For a recent review: Q. Xia, J. Dong, H. Song, Q. Wang, *Chem. Eur. J.* **2019**, *25*, 2949 – 2961.

[56] K. T. Tarantino, P. Liu, R. R. Knowles, *J. Am. Chem. Soc.* **2013**, *135*, 10022 – 10025.

[57] A. N. Butkevich, M. L. Bossi, G. Lukinavicius, S. W. Hell, *J. Am. Chem. Soc.,* **2019**, *141*, 981–989.

[58] F. Miomandre, P. Audebert, K. Zong, J. R. Reynolds, *Langmuir*, **2003**, *19*, 8894-8898.

[59] Y. Zhao, D. G. Truhlar*, Theor. Chem. Acc.* **2008**, *120*, 215-224.

[60] C. Wang, Q. Qiao, W. Chi, J. Chen, W. Liu, D. Tan, S. McKechnie, D. Lyu, X.-F. Jiang, W. Zhou, N. Xu, Q. Zhang, Z. Xu, X. Liu *Angew. Chem.* **2020**, 132, 10246-10258; *Angew. Chem. Int. Ed.* **2020**, *59*, 10160-10172.

[61] X. Liu, Q. Qiao, W. Tian, W. Liu, J. Chen, M. J. Lang, Z. Xu, *J. Am. Chem. Soc.* **2016**, *138*, 6960−6963.